



Cite this: *Chem. Commun.*, 2014, 50, 14873

Received 22nd July 2014,
Accepted 19th September 2014

DOI: 10.1039/c4cc05687f

www.rsc.org/chemcomm

A single-chain magnet based on linear $[\text{Mn}^{\text{III}}_2\text{Mn}^{\text{II}}]$ units†

Constantina Papatriantafyllopoulou,^a Sotiris Zartilas,^a Manolis J. Manos,^{‡a}
Céline Pichon,^{bc} Rodolphe Clérac^{*bc} and Anastasios J. Tasiopoulos^{*a}

The synthesis, structural characterization and magnetic properties of a 1D coordination polymer based on a linear mixed valent $[\text{Mn}^{\text{III}}_2\text{Mn}^{\text{II}}]$ repeating unit are described. It displays single-chain magnet (SCM) behaviour with an energy barrier of ~ 38 K and represents the first example of a mixed valent Mn–carboxylate SCM with a linear architecture.

Polynuclear Mn–carboxylate complexes and coordination polymers have attracted intense interest due to numerous reasons including their novel crystal structures and interesting magnetic properties.¹ Such compounds often behave as single-molecule magnets (SMMs) or single-chain magnets (SCMs) displaying novel magnetic phenomena such as slow relaxation, large hysteresis and quantum tunneling of magnetisation (QTM).^{1–4} SMMs derive their properties from the combination of a large spin ground-state and Ising-type (easy-axis) magnetic anisotropy whereas SCMs possess strong intrachain exchange interactions without spin compensation between high spin anisotropic (Ising-type) units along the chain.^{1–3} Such magnetic species are remarkable results of the molecular approach to nano-scale magnetic materials and have been proposed as candidates for applications in high-density information storage, molecular spintronics and quantum computation.⁵

As a result, numerous Mn–carboxylate complexes and SMMs have been reported with a variety of topologies and nuclearities ranging from 2 to 84,^{1,6} but in contrast, only a small number of homospin manganese SCMs have been described.² The largest category of Mn complexes in the field of molecular magnetism

is possibly the trinuclear species since they often display ferromagnetic exchange interactions and SMM behaviour.^{1d,7} Such $[\text{Mn}_3]$ units have also been used as building blocks or modules for the construction of larger aggregates^{1d,8} and multi-dimensional coordination polymers, which display interesting magnetic properties.^{1d,9} Thus, several $[\text{Mn}_3]$ SMMs and a few $[\text{Mn}_3]_\infty$ SCMs have been reported with the vast majority of these materials being based on oxido-centered triangular topology.^{1d,7–9}

To the best of our knowledge, there are only four linear $[\text{Mn}_3]$ complexes that have been reported to exhibit SMM behaviour,¹⁰ whereas such moieties have never been observed to form SCM systems. In fact, SCMs consisting of linear polynuclear Mn–carboxylate repeating units are completely unknown. These simple 1D architectures built from linear modules are particularly interesting since they provide ideal model systems,^{2a,b} which could become textbook examples for magnetochemists and physicists, allowing them to go further in the understanding of the SCM theory. Although SCMs with linear architectures are well known when rigid ligands that impose the geometry of the resultant compounds, such as cyanides,¹¹ are employed, they are very rare in 3d metal carboxylate chemistry.^{12,13}

We herein report the synthesis, crystal structure and magnetic properties of an 1D coordination polymer $[\text{Mn}_3(\text{mpt})_2(\text{EtCO}_2)_2(\text{MeOH})_2]_\infty$ (**1**)_∞ (H_3mpt : 3-methylpentane-1,3,5-triol), based on a novel linear mixed valent trinuclear $[\text{Mn}^{\text{III}}_2\text{Mn}^{\text{II}}]$ repeating unit. It displays SCM properties with a thermally activated relaxation time and an energy barrier of about 38 K. This compound represents not only the first example of a SCM based on a linear Mn_x –carboxylate repeating unit but also the first mixed valent Mn–carboxylate SCM with a linear architecture.

The solvothermal reaction of $\text{Mn}(\text{O}_2\text{CET})_2 \cdot 2\text{H}_2\text{O}$ and H_3mpt in a $\sim 1:2$ molar ratio in MeOH at 100 °C for 24 h followed by slow cooling to room temperature gave brown rod-shaped crystals of (**1**)_∞ in 35% yield; the dried solid was analysed satisfactorily as (**1**)_∞§ (for synthetic details see the ESI†). The crystal structure§ of (**1**)_∞ contains an 1D coordination polymer consisting of a linear trinuclear $[\text{Mn}_3(\text{mpt})_2(\text{EtCO}_2)_2(\text{MeOH})_2]$ (Fig. 1, top) repeating unit. Charge considerations, bond valence

^a Department of Chemistry, University of Cyprus, 1678 Nicosia, Cyprus; E-mail: atasio@ucy.ac.cy; Fax: +357 22892801; Tel: +357 22892765

^b CNRS, CRPP, UPR 8641, F-33600 Pessac, France.

E-mail: clerac@crpp-bordeaux.cnrs.fr

^c Univ. Bordeaux, CRPP, UPR 8641, F-33600 Pessac, France

† Electronic supplementary information (ESI) available: Crystallographic data (CIF format) for (**1**)_∞ and various structure and magnetism figures. CCDC 1015476. For the ESI and crystallographic data in CIF or other electronic format see DOI: 10.1039/c4cc05687f

‡ Current address: Department of Chemistry, University of Ioannina, 45110, Ioannina, Greece.



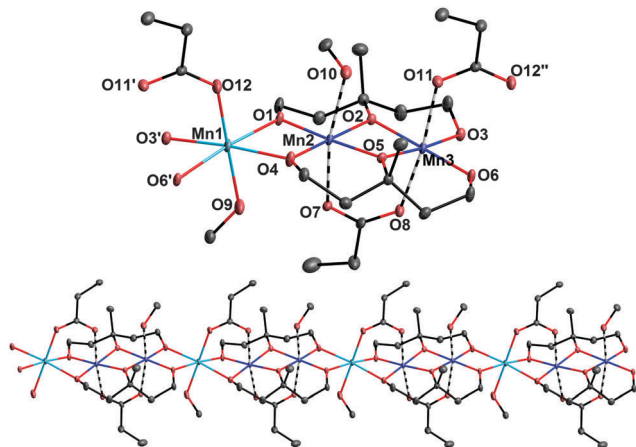


Fig. 1 ORTEP-like view of the repeating unit (top) and a part of the one-dimensional structure of $(\mathbf{1})_\infty$ (bottom) with thermal ellipsoids fixed at 50%. Colour code: Mn^{II}, cyan; Mn^{III}, blue; O, red; C, grey. The H atoms are omitted for clarity. The Mn^{III} Jahn–Teller axes are indicated by dashed bonds.

sum calculations¹⁴ and inspection of metric parameters indicate that the $[\text{Mn}_3]$ moiety is mixed-valent containing two Mn^{III} (Mn2 and Mn3) and one Mn^{II} (Mn1) ions with the latter located in the one outer part of the linear $[\text{Mn}_3]$ unit.

The three Mn ions are held together by one EtCO_2^- group bridging in the usual *syn, syn* - $\eta^1: \eta^1: \mu$ fashion the two Mn^{III} ions and two $\eta^2: \eta^2: \eta^2: \mu_4$ mpt³⁻ ligands. Two μ -OR arms of the latter together with an additional *syn, syn* - $\eta^1: \eta^1: \mu$ EtCO_2^- group link the neighbouring $[\text{Mn}_3]$ units resulting in the formation of the 1D coordination polymer of $(\mathbf{1})_\infty$ (Fig. 1, bottom). The Mn^{III}–O–Mn^{III} and Mn^{III}–O–Mn^{II} angles are $\sim 98.4(2)^\circ$ and $\sim 100.5(2)^\circ$, respectively, whereas the Mn^{III}–O–Mn^{II} angle between the neighbouring units of $(\mathbf{1})_\infty$ is $\sim 97.1(2)^\circ$. The peripheral ligation is completed by two terminal methanol molecules connected to the central Mn^{III} (Mn2) and Mn^{II} ions. The Mn ions are in very close proximity along the chain, with Mn···Mn separations of 3.120, 2.904 and 3.038 Å for Mn1···Mn2, Mn2···Mn3 and Mn3···Mn1, respectively. All Mn ions are six-coordinated adopting a distorted octahedral geometry with the two Mn^{III} ions displaying the expected Jahn–Teller elongation axes (O7–Mn2–O10 and O8–Mn3–O11) which are nearly co-parallel (the angle between the JT axes is $\sim 7.6(1)^\circ$). These JT axes involve donor atoms either from methanol or propionate ligands, and thus all equatorial coordinating positions of the Mn^{III} ions are occupied by the alkoxido O atoms of the two mpt³⁻ ligands. It is also noticeable that the Mn ions within the chain are nearly co-linear with intrachain Mn–Mn–Mn angles being in the 170° – 180° range. Examination of the crystal packing reveals that the chains run parallel to the *a* axis and there is no significant interchain hydrogen bonding interactions (Fig. S1, ESI[†]). Thus, the neighbouring chains are well separated, with the interchain Mn···Mn separations all being superior to 8.27 Å.

The 1D coordination polymer found in $(\mathbf{1})_\infty$ displays several attractive and unique structural features. In particular, $(\mathbf{1})_\infty$ is the first example of a coordination polymer, and a rare example of a metal complex in general, containing the H_3mpt ligand in its neutral or anionic form.¹⁵ In addition, its structural

architecture that can be described as a linear array of Mn²⁺ and Mn³⁺ ions tightly connected through both mono- and poly-atomic bridges (RO^- and EtCO_2^- respectively), is unprecedented in Mn–carboxylate chemistry, although some chains consisting of mononuclear repeating units have been reported.^{12,16} Such compounds, especially those containing one or more trivalent Mn ions like $(\mathbf{1})_\infty$, are particularly attractive in the area of molecular magnetism since they could display SCM properties induced by the intrinsic magnetic anisotropy of their Mn^{III} centers.

The magnetic properties of $(\mathbf{1})_\infty$ were investigated as a function of temperature (1.8–270 K) using dc magnetic fields up to 7 T. A plot of χT versus T for $(\mathbf{1})_\infty$, recorded at 1000 Oe, is shown in Fig. 2. The χT value steadily decreases from $7.9 \text{ cm}^3 \text{ mol}^{-1} \text{ K}$ at 270 K to $4.7 \text{ cm}^3 \text{ mol}^{-1} \text{ K}$ at 34 K and then rapidly increases to $6.8 \text{ cm}^3 \text{ mol}^{-1} \text{ K}$ at 4 K before it drops down to $5.5 \text{ cm}^3 \text{ mol}^{-1} \text{ K}$ at 1.85 K. The room temperature χT product is significantly smaller than the spin-only ($g = 2$) value of $10.375 \text{ cm}^3 \text{ mol}^{-1} \text{ K}$ expected for one Mn^{II} and two Mn^{III} non-interacting centers. The overall profile of the χT versus T plot for $(\mathbf{1})_\infty$ reveals the existence of competing ferromagnetic and antiferromagnetic exchange interactions within the chain, the latter being responsible for the low χT product at 270 K. The χT value around 40 K suggests a virtual spin ground state (S_T) of 5/2 for the $[\text{Mn}^{\text{III}}_2\text{Mn}^{\text{II}}]$ repeating unit induced by significant antiferromagnetic interactions while the increase below 40 K reveals probably ferromagnetic interactions between these trinuclear magnetic moieties. The decrease of the χT value below 4 K is likely due to the existence of weak antiferromagnetic interchain interactions, magnetic anisotropy and Zeeman effects from the applied field.

In order to quantify the strength of the intrachain interactions in $(\mathbf{1})_\infty$, the magnetic susceptibility was modeled using the following classical spin chain Hamiltonian:

$$\mathbf{H} = -2 \sum_{i=1}^N J_1 (\vec{S}_{1,i} \cdot \vec{S}_{A,i}) + J_2 (\vec{S}_{A,i} \cdot \vec{S}_{B,i}) + J_1' (\vec{S}_{B,i} \cdot \vec{S}_{1,i+1})$$

with J_1 and J_1' being the two different Mn^{II}–Mn^{III} magnetic interactions, J_2 being the Mn^{III}–Mn^{III} coupling, $S_{1,i} = 5/2$ and

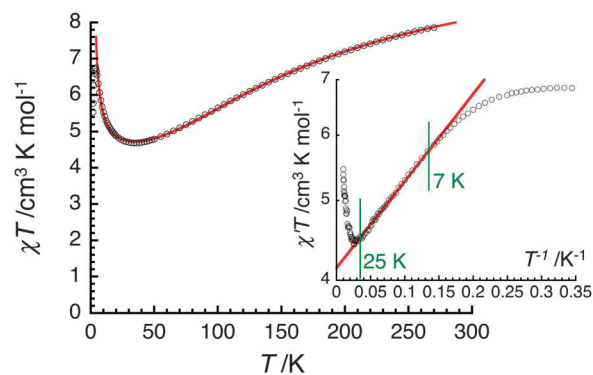


Fig. 2 Temperature dependence of the χT product (χ is the magnetic susceptibility per mole of $[\text{Mn}_3]$ unit at 1000 Oe) between 1.8 and 270 K for a polycrystalline sample of $(\mathbf{1})_\infty$ (Fig. S2, ESI[†]). The solid red line is the best fit of the experimental data to the chain model (see text). Inset: the semi-logarithmic $\chi' T$ versus T^{-1} plot (χ' being the in-phase ac susceptibility in zero dc field at 100 Hz and $H_{\text{ac}} = 3$ Oe) with the best fit (red solid line) using the 1D Ising model between 7 and 25 K.



$S_{A,i} = S_{B,i} = 2$. Fisher's approach¹⁷ was extended to establish an analytical expression of the low field susceptibility of this 1D system (see ESI†). Between 5 and 270 K, an excellent fit of the experimental data was obtained with $J_1/k_B = -11(1)$ K, $J_2/k_B = -20(1)$ K, $J_1'/k_B = +0.23(5)$ K and $g = 2.00(5)$ (Fig. 2).¹⁸ The existence of moderate antiferromagnetic exchange for the $[\text{Mn}^{\text{III}}(\mu\text{-OR})_2(\text{O}_2\text{CET})\text{Mn}^{\text{III}}]$ unit with the two ($\mu\text{-OR}$) arms in the equatorial position is in perfect accordance with results reported for analogous systems.¹⁹ On the other hand, it is very difficult to assign the J_1 and J_1' interactions to the $[\text{Mn}^{\text{III}}(\mu\text{-OR})_2(\text{O}_2\text{CET})\text{Mn}^{\text{II}}]$ or $[\text{Mn}^{\text{II}}(\mu\text{-OR})_2\text{Mn}^{\text{III}}]$ pathways. Although, it is tempting to assume that the former one is ferromagnetic due to more acute Mn^{III}–O–Mn^{II} angles (97.1° versus 100.5°), the facts that the two units are different and also that there has been no magnetostructural study on such linkages with similar metric parameters do not allow us to confidently conclude on the assignment.^{10a,20} But in both cases, this magnetic system can be viewed at low temperatures as a chain of $S_T = 5/2$ $[\text{Mn}^{\text{III}}_2\text{Mn}^{\text{II}}]$ units with weak ferromagnetic interactions. In order to further test the 1D nature of the magnetic properties of $(1)_\infty$, the temperature dependence of the correlation length, ξ , was estimated from the magnetic susceptibility. In any 1D classical systems, ξ is directly proportional to $\chi'T$ (χ' being the zero field susceptibility).^{2a,17,21} For an Ising-like or anisotropic Heisenberg spin chain, the $\chi'T$ product follows a thermally activated behaviour: $\chi'T \approx C_{\text{eff}} \times \exp(\Delta\xi/k_B T)$ (C_{eff} : the effective Curie constant; $\Delta\xi$: the energy to create a domain wall along the chain).^{2a} Confirming the 1D Ising-like character of the magnetic properties, the $\ln(\chi'T)$ versus $1/T$ plot (inset Fig. 2) features a linear region between 7 and 25 K with $\Delta\xi$ equal to 2.5 K. Notably, $\Delta\xi$ is smaller (but still of the same order of magnitude) than the theoretical value in the Ising limit:^{2a} $\Delta\xi/k_B = 4J_{\text{eff}}S_T^2/k_B = 4.6 \pm 1$ K (with $J_{\text{eff}}S_T^2 = J_1'S_1S_A$). The reduction of $\Delta\xi$ is likely induced by low lying excited states above the $S_T = 5/2$ ground state and also by a possible departure from the Ising limit. Nevertheless, the 1D magnetic properties of $(1)_\infty$ are clearly established. In addition, due to the presence of non-compensated spins along the chain, which is also composed of anisotropic repeating units, all the ingredients seem to be present in $(1)_\infty$ to observe a SCM behaviour.^{2a,c} Therefore, even if the M versus H data (Fig. S3, ESI†) did not show any sign of hysteresis effect (at 100–400 Oe min^{-1}), ac susceptibility measurements were performed to probe the magnetisation dynamics. The ac data, shown in Fig. 3, reveal a strong frequency dependence of both in-phase (χ') and out-of-phase (χ'') signals below 4 K indicating the existence of slow relaxation of magnetisation in $(1)_\infty$. The temperature dependence of the magnetisation relaxation time, τ , was deduced from the out-of-phase data (versus T and ν) as shown in the inset of Fig. 3.

The τ versus $1/T$ data were fitted to the Arrhenius equation $\tau = \tau_0 \exp(\Delta\tau/k_B T)$ (where $\Delta\tau$ is the energy barrier to reverse the magnetisation of a chain and τ_0 is the intrinsic reversal time of the magnetically isolated spin unit of the chain in contact with the thermal bath) with $\Delta\tau/k_B = 38$ K and $\tau_0 = 8.0 \times 10^{-11}$ s, the latter value being in good agreement with those of reported SCMs.^{2,11,12} Considering that the correlation length, ξ , ($\propto \chi'T$) is saturating around 3 K (Fig. 2), the observed dynamics of magnetisation (below 3 K; Fig. 3) have been measured in the finite-size regime of SCM relaxation.^{2a,c} Therefore the anisotropy

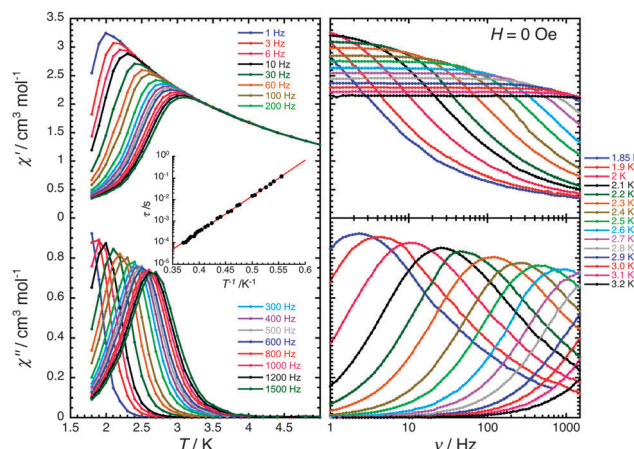


Fig. 3 Temperature (1.86–5 K; left) and frequency (1–1500 Hz; right) dependence of the real (χ' , top) and imaginary (χ'' , bottom) parts of the ac susceptibility for $(1)_\infty$ in zero dc-field (with $H_{\text{ac}} = 3$ Oe). Solid lines are visual guides. Inset: relaxation time (τ) versus T^{-1} plot in zero dc-field for $(1)_\infty$. The red solid line is the fit to the Arrhenius law.

barrier (Δ_A) can be estimated at 35.5 K from $\Delta\xi$ and $\Delta\tau$, as in this regime $\Delta\tau = \Delta\xi + \Delta_A$. This significant value of the magnetic anisotropy energy is in good agreement with the lack of saturation of magnetisation at fields up to 7 T (Fig. S3, ESI†).

In conclusion, the use of the triol H_3mpt in Mn–carboxylate chemistry afforded a 1D coordination polymer, $(1)_\infty$, consisting of tightly connected $[\text{Mn}^{\text{III}}_2\text{Mn}^{\text{II}}]$ linear repeating units. For only the second time in the family of Mn–carboxylate chains with a linear structural architecture and the first time for mixed valent ones, this system exhibits SCM properties with an appreciable relaxation energy barrier of 38 K. It should also be pointed out that the mpt^{3-} ligand plays a crucial role not only in the formation but also in the appearance of SCM behaviour in $(1)_\infty$. In particular, its alkoxido bridging arms occupied all equatorial positions of the Mn ions directing the terminal solvent and carboxylate ligands to the axial ones thus contributing to the alignment of the local easy magnetic axes of the Mn^{III} ions along the chain direction. Thus, this work reveals that H_3mpt could be a valuable ligand for the isolation of novel carboxylate-based SCMs with simple spin and interaction topologies.

This work was supported by the European Union Seventh Framework Programme (FP7/2007–2013) under grant agreement no. PCIG09-GA-2011-293814, the Cyprus Research Promotion Foundation (PENEK-EVIX/0506/08), the University of Bordeaux, the ANR, the Région Aquitaine, and the CNRS.

Notes and references

§ Vacuum-dried solid analysed (C and H) as $(1)_\infty$. Calcd (found): C, 37.69 (37.82) and H, 6.33 (6.01)%. Crystal data for $(1)_\infty$: $\text{C}_{20}\text{H}_{40}\text{Mn}_3\text{O}_{12}$, $M_w = 637.34$ g mol^{-1} , triclinic space group $P\bar{1}$, $a = 9.0326(8)$ Å, $b = 9.208(2)$ Å, $c = 17.277(2)$ Å, $\alpha = 102.92(2)^\circ$, $\beta = 91.393(9)^\circ$, $\gamma = 111.20(1)^\circ$, $Z = 2$, $V = 1297.0(3)$ Å³, $T = 100(2)$ K, $\rho_{\text{calcd}} = 1.632$ g cm^{-3} , 7567 reflections collected, 3361 reflections used, $R_1 [I > 2\sigma(I)] = 0.0476$, $wR_2 = 0.1410$.

- (a) R. Bagai and G. Christou, *Chem. Soc. Rev.*, 2009, **38**, 1011;
- (b) G. Aromi and E. K. Brechin, *Struct. Bonding*, 2006, **122**, 1;
- (c) A. J. Tasiopoulos and S. P. Perlepes, *Dalton Trans.*, 2008, 5537;



- (d) R. Inglis, C. J. Milios, L. F. Jones, S. Piligkos and E. K. Brechin, *Chem. Commun.*, 2012, **48**, 181.
- 2 (a) C. Coulon, H. Miyasaka and R. Clérac, *Struct. Bonding*, 2006, **122**, 163; (b) I.-R. Jeon and R. Clérac, *Dalton Trans.*, 2012, 9569; (c) H. Miyasaka, M. Julve, M. Yamashita and R. Clérac, *Inorg. Chem.*, 2009, **48**, 3420; (d) K. Bernot, J. Luzon, R. Sessoli, A. Vindigni, J. Thion, S. Richeter, D. Leclercq, J. Larionova and A. Van der Lee, *J. Am. Chem. Soc.*, 2008, **130**, 1619; (e) T.-T. Wang, M. Ren, S.-S. Bao, B. Liu, L. Pi, Z.-S. Cai, Z.-H. Zheng, Z.-L. Xu and L.-M. Zheng, *Inorg. Chem.*, 2014, **53**, 3117.
- 3 D. Gatteschi and R. Sessoli, *Angew. Chem., Int. Ed.*, 2003, **42**, 268.
- 4 (a) J. R. Friedman, M. P. Sarachik, J. Tejada and R. Ziolo, *Phys. Rev. Lett.*, 1996, **76**, 3830; (b) L. Thomas, F. Lioni, R. Ballou, D. Gatteschi, R. Sessoli and B. Barbara, *Nature*, 1996, **383**, 145; (c) W. Wernsdorfer, R. Clérac, C. Coulon, L. Lecren and H. Miyasaka, *Phys. Rev. Lett.*, 2005, **95**, 237203.
- 5 (a) L. Bogani and W. Wernsdorfer, *Nat. Mater.*, 2008, **7**, 179; (b) M. N. Leuenberger and D. Loss, *Nature*, 2001, **410**, 789.
- 6 (a) G. E. Kostakis, A. M. Ako and A. K. Powell, *Chem. Soc. Rev.*, 2010, **39**, 2238; (b) A. J. Tasiopoulos, A. Vinslava, W. Wernsdorfer, K. A. Abboud and G. Christou, *Angew. Chem., Int. Ed.*, 2004, **43**, 2117.
- 7 (a) T. C. Stamatatos, D. Foguet-Albiol, C. C. Stoumpos, C. P. Raptopoulou, A. Terzis, W. Wernsdorfer, S. P. Perlepes and G. Christou, *J. Am. Chem. Soc.*, 2005, **127**, 15380; (b) T. C. Stamatatos, D. Foguet-Albiol, S.-C. Lee, C. C. Stoumpos, C. P. Raptopoulou, A. Terzis, W. Wernsdorfer, S. O. Hill, S. P. Perlepes and G. Christou, *J. Am. Chem. Soc.*, 2007, **129**, 9484; (c) C.-I. Yang, W. Wernsdorfer, K.-H. Cheng, M. Nakano, G.-H. Lee and H.-L. Tsai, *Inorg. Chem.*, 2008, **47**, 10184.
- 8 (a) E. K. Brechin, *Chem. Commun.*, 2005, 5141; (b) T. N. Nguyen, W. Wernsdorfer, K. A. Abboud and G. Christou, *J. Am. Chem. Soc.*, 2011, **133**, 20688; (c) B. Cordero, O. Roubeau, S. J. Teat and A. Escuer, *Dalton Trans.*, 2011, **40**, 7127; (d) A. M. Mowson, T. N. Nguyen, K. A. Abboud and G. Christou, *Inorg. Chem.*, 2013, **52**, 12320.
- 9 (a) Y.-L. Bai, J. Tao, W. Wernsdorfer, O. Sato, R.-B. Huang and L.-S. Zheng, *J. Am. Chem. Soc.*, 2006, **128**, 16428; (b) C. M. Liu, D.-Q. Zhang and D.-B. Zhu, *Inorg. Chem.*, 2009, **48**, 4980; (c) H.-B. Xu, B.-W. Wang, F. Pan, Z. Wang and S. Gao, *Angew. Chem., Int. Ed.*, 2007, **46**, 7388.
- 10 (a) A. Prescimone, J. Wolowska, G. Rajaraman, S. Parsons, W. Wernsdorfer, M. Murugesu, G. Christou, S. Piligkos, E. J. L. McInnes and E. K. Brechin, *Dalton Trans.*, 2007, 5282; (b) P.-H. Lin, S. Gorelsky, D. Savard, T. J. Burchell, W. Wernsdorfer, R. Clérac and M. Murugesu, *Dalton Trans.*, 2010, **39**, 7650; (c) C.-L. Zhou, Z.-M. Wang, B.-W. Wang and S. Gao, *Dalton Trans.*, 2012, **41**, 13620; (d) F. Habib, G. Brunet, F. Loiseau, T. Pathmalingam, T. J. Burchell, A. M. Beauchemin, W. Wernsdorfer, R. Clérac and M. Murugesu, *Inorg. Chem.*, 2013, **52**, 1296.
- 11 (a) H. Miyasaka, T. Madanbashi, A. Saitoh, N. Motokawa, R. Ishikawa, M. Yamashita, S. Bahr, W. Wernsdorfer and R. Clérac, *Chem. – Eur. J.*, 2012, **18**, 3942; (b) X. Feng, T. D. Harris and J. R. Long, *Chem. Sci.*, 2011, **2**, 1688; (c) T. D. Harris, M. V. Bennett, R. Clérac and J. R. Long, *J. Am. Chem. Soc.*, 2010, **132**, 3980.
- 12 A. V. Prosvirin, H. Zhao and K. R. Dunbar, *Inorg. Chim. Acta*, 2012, **389**, 118.
- 13 (a) X. N. Cheng, W. Xue, W.-X. Zhang and X.-M. Chen, *Chem. Mater.*, 2008, **20**, 5345; (b) D.-R. Xiao, G.-J. Zhang, J.-L. Liu, L.-L. Fan, R. Yuan and M.-L. Tong, *Dalton Trans.*, 2011, **40**, 5680; (c) Y.-Z. Zheng, W. Xue, M. L. Tong, X.-M. Chen, F. Grandjean and J. J. Long, *Inorg. Chem.*, 2008, **47**, 4077.
- 14 (a) Bond Valence Sum calculations gave oxidation state values of 1.99 (Mn^{II}) and 3.00/3.01 (Mn^{III}) for the Mn ions of (1)_∞^{14b}; (b) W. Liu and H.-H. Thorp, *Inorg. Chem.*, 1993, **32**, 4102.
- 15 (a) S. Nayak, M. Evangelisti, A. K. Powell and J. Reedijk, *Chem. – Eur. J.*, 2010, **16**, 12865; (b) S. Zartilas, C. Papatriantafyllopoulou, T. C. Stamatatos, V. Nastopoulos, E. Cremades, E. Ruiz, G. Christou, C. Lampropoulos and A. J. Tasiopoulos, *Inorg. Chem.*, 2013, **52**, 12070; (c) M. Charalambous, S. Z. Zartilas, E. E. Moushi, C. Papatriantafyllopoulou, M. J. Manos, T. C. Stamatatos, S. Mukherjee, V. Nastopoulos, G. Christou and A. J. Tasiopoulos, *Chem. Commun.*, 2014, **50**, 9090.
- 16 (a) A. J. Tasiopoulos, N. C. Harden, K. A. Abboud and G. Christou, *Polyhedron*, 2003, **22**, 133; (b) D. J. Price, S. R. Batten, B. Moubaraki and K. S. Murray, *Polyhedron*, 2003, **22**, 2161; (c) A. J. Tasiopoulos, W. Wernsdorfer, K. A. Abboud and G. Christou, *Inorg. Chem.*, 2005, **44**, 6324.
- 17 M. E. Fisher, *Am. J. Phys.*, 1964, **32**, 343.
- 18 When $J_1 = J_1'$ is imposed in the fitting procedure, it is impossible to reproduce the experimental data in a satisfactory manner.
- 19 (a) C. Palopoli, M. González-Sierra, G. Robles, F. Dahan, J.-P. Tuchagues and S. Signorella, *J. Chem. Soc., Dalton Trans.*, 2002, 3813; (b) N. Berg, T. Rajeshkumar, S. M. Taylor, E. K. Brechin, G. Rajaraman and L. F. Jones, *Chem. – Eur. J.*, 2012, **18**, 5906.
- 20 (a) D. Mandal, P. B. Chatterjee, S. Bhattacharya, K.-Y. Choi, R. Clérac and M. Chaudhury, *Inorg. Chem.*, 2009, **48**, 1826; (b) A. R. Schake, E. A. Schmitt, A. J. Conti, W. E. Streib, J. C. Huffman, D. N. Hendrickson and G. Christou, *Inorg. Chem.*, 1991, **30**, 3192; (c) S. Gou, Q. Zeng, Z. Yu, M. Qian, J. Zhu, C. Duan and X. You, *Inorg. Chim. Acta*, 2000, **303**, 175.
- 21 A general demonstration of the relationship between the correlation length and the zero-field magnetic susceptibility is reported by Fisher in ref. 17 (before applying to the classical Heisenberg model).

